Electronic structure of Cu-Au alloys from the Cu perspective: A Cu $L_{3,2}$-edge study

T. K. Sham

Department of Chemistry, The University of Western Ontario, London N6A 5B7, Canada

A. Hiraya* and M. Watanabe[†]

UVSOR, Institute for Molecular Science, Okazaki, 44 Japan

(Received 7 August 1996; revised manuscript received 1 October 1996)

We have obtained Cu $L_{3,2}$-edge x-ray-absorption near-edge structures (XANES) for a series of Cu-Au alloys. It is found that all samples exhibit a three-peak pattern at the Cu L_3 edge within the first 10 eV above the threshold. Close examination reveals chemical systematics in the position of the threshold and of the resonance maxima and in the intensity of the resonances. These results are used to infer charge redistribution at the Cu site. They are compared with previous studies of the same alloys from the Au perspective and with theoretical calculations. Comparisons between the ordered and disordered phase of Cu_3Au and CuAu, and the Cu $L_{3,2}$- and K-edge XANES are also made. Our study strongly indicates that d-charge redistribution at the Cu and Au sites is in the opposite direction upon alloy formation; that is, relative to the pure element, Au loses d charge and Cu gains d charge and charge transfer is sensitive to the number of nearest neighbors of unlike atoms. [S0163-1829(97)03812-5]

I. INTRODUCTION

Although there has been extensive literature of Cu-Au alloys, their electronic structures continue to be an interesting subject for both experimental and theoretical investigation. This is partly because of the availability of better tools in both experimental[1–3] and computational[4–20] techniques and partly because of the need for detailed understanding of this prototypical system, which, in addition to being a classical case for order-disorder phase transition, provides a basis for the studies of bimetallic interactions in systems of unusual dimensions such as two-dimensional alloys,[21–30] bimetallic interface,[31,32] supported mixed metal clusters,[33] and nanostructures.[34]

Experimental studies of the electronic structure of Au-Cu alloys concerning charge redistribution have been traditionally concentrated on the Mössbauer effect[35–37] and photoemission.[38–43] These techniques take advantage of a Mössbauer nucleus Au^{197}, a narrow Au $4f$ level, and a chemically sensitive $5d$ band. More recently, a Au L-edge x-ray-absorption near-edge structure (XANES) was used to probe the unoccupied densities of d states above the Fermi level in bulk Cu-Au alloys.[44,45] Thus most of the information obtained from these studies inevitably focused on the Au site. Information on the Cu site in Au-Cu alloys is often obtained from the Cu $2p$ shifts and the valence-band photoemission spectrum as well as indirectly from the Au results taking into account electronegativity and electroneutrality considerations.[44,45] It has been shown that Au loses d electron charge upon alloying and this loss is overcompensated by non-d conduction electron gain.[45] The net charge flow is small ($\sim 0.1e$) and is onto Au (the site is defined by the Wigner-Seitz volume), in good accord with electronegativity (Au is the most electronegative metallic element) and electroneutrality (atomic sites in a metallic alloy tend to maintain electroneutrality locally) arguments. This charge compensation mechanism (rehybridization)[38] appears to be quite general for binary Au alloys[46] and has been confirmed for Au-Cu alloys by a Au $L_{3,2}$-edge study that shows that at the Au site, the ratio of the change in s vs d charge count $\Delta n_d / \Delta n_s = -0.7$ remains essentially constant.[45] The charge redistribution picture at the Cu site is less clear, although charge conservation demands that the less electronegative Cu would lose net charge overall and the photoemission Cu $2p$ core-level shift indicates that Cu probably gains d charge.[45] Thus Cu would have to lose non-d (s and p) charge to be in accord with electronegativity considerations. It is clear that experiments focusing on the Cu site are needed for the clarification of the redistribution of the valence electrons of Cu in Cu-Au alloy formation.

In this paper, we report a Cu $L_{3,2}$-edge XANES study for a series of Cu-Au alloys with emphasis on probing the electronic structure at the Cu site. Since the Cu $L_{3,2}$ edge probes primarily the unoccupied densities of states of $3d$ character (dipole selection rule with $p \rightarrow d$ transition being the dominant one), it will provide information concerning the role of the Cu $3d$ electrons in Cu-Au alloy formation. It should be noted that synchrotron light is required for these studies and for a long time, high-resolution beam lines covering the soft-x-ray photon energy region in the vicinity of 1 keV (Cu L_3 edge is at $\sim$930 eV) were relatively few comparing to its hard-x-ray counterparts. Most of the XANES data for the L edge of Cu and the first-row transition metals were obtained with electron-energy-loss spectroscopy.[47,48] It was not until recently that high-resolution photons in this energy range became more readily available.[49] This is partly because of the intrinsic difficulties in the choice of monochromators (neither crystals nor gratings were considered ideal in this region) and partly because of the fact that this energy region falls between the emphasis of high-energy storage rings (x rays) and low-energy storage rings (vacuum ultraviolet). We show below that with high resolution, which reveals the fine structures of the XANES, chemical systematics of the change in the electronic structure associated with alloying

are observed and, together with previous results focused on the Au site and theoretical calculations, the XANES systematics can be correlated with charge redistribution at the Cu site; that is, Cu gains a d and loses an s electron upon compound formation. The sensitivity of the technique is also noted.

II. EXPERIMENT

Alloy samples $Cu_{0.75}Au_{0.25}$, $Cu_{0.5}Au_{0.5}$, and $Cu_{0.25}Au_{0.75}$, henceforth denoted Cu_3Au, CuAu, and $CuAu_3$, respectively, were used in this study. These samples were prepared by repeatedly quenching from the melt stoichiometric amount of the pure constituents as described previously.[45] The as-prepared samples are polycrystalline random alloys and are referred to as disordered. The ordered compounds were prepared by annealing the disordered sample in inert atmosphere just below the phase transition temperature for several weeks. The structural aspects of ordered and disordered phases of these alloys have been studied by Au L_3-edge extended x-ray-absorption fine-structure studies.[45,50]

Cu $L_{3,2}$-edge XANES measurements were carried out using the BL1A double-crystal monochromator (DXM) beam line[51] at UVSOR, Institute for Molecular Science, Okazaki, Japan. The operating current of the 750-MeV storage ring was 200 mA at injection. Beryl crystals ($2d$ = 15.965 Å) were used to provide monochromatic photons with a flux of 10^8–10^9 photon/sec and an overall resolution less than 0.9 eV at the Cu L_3 edge (~930 eV). All Cu $L_{3,2}$-edge XANES spectra were recorded simultaneously in both total electron yield (TEY) and fluorescence yield (FLY) modes with the specimen mounted on a sample manipulator in a vacuum chamber as described previously.[52] The TEY was recorded with the specimen current as well as a channel plate electron multiplier. The FLY was recorded with a proportional counter filled with a Ar-CH$_4$ gas mixture. The surface of the specimens was cleaned by scraping *in situ* with a diamond file. This procedure removes the inadvertent surface contaminants and native oxides and is crucial for total electron yield measurements since the TEY technique has a shallow sampling depth.[53] The fluorescence yield, on the other hand, has a much deeper sampling depth and is dominated by the bulk signal.[54] Despite its bulk sensitivity, the FLY suffers from self-absorption for concentrated samples, low count rates, and low signal to noise ratio. Thus simultaneous XANES measurements using both TEY and FLY techniques ensure that the spectra obtained are of good quality and representative of bulk properties.[53] All the results reported here were obtained from TEY measurements for better statistics. The corresponding FLY spectra were used to ensure surface cleanliness.

III. RESULTS

Figure 1 shows the Cu $L_{3,2}$-edge XANES of the disordered alloys $CuAu_3$, CuAu, and $CuAu_3$ together with Cu metal and CuO. The monochromator was calibrated using the Cu L_3-edge resonance maximum in CuO (931.06 eV).[34] The point of inflection at the Cu L_3 edge of the pure Cu metal (E_0) thus obtained appears at 932.40 eV. In the alloy TEY XANES, there sometimes exists a small surface oxide
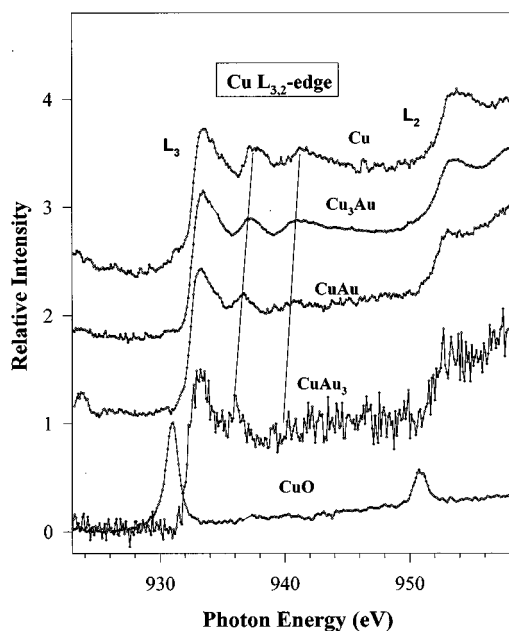

FIG. 1. Cu $L_{3,2}$-edge XANES Cu metal and a series of disordered Cu-Au alloys; XANES for CuO is also shown for comparison.

peak due to the incomplete removal of surface oxide, which is not seen in the FLY spectrum. The oxide contribution can be removed by subtracting from the spectrum a scaled CuO spectrum. Since CuO is featureless above the threshold, this procedure has no noticeable effect on the position and relative intensity of the XANES resonances above the threshold.

Several features from Fig. 1 are apparent. First, all the spectra exhibit three similar resonances above the Cu L_3 edge. Second, close inspection reveals that the threshold E_0 of the alloys shifts to lower photon energy as Cu becomes more dilute in Au. Third, there are systematic variations in the resonance position and intensity; that is, the resonance intensity decreases and the maximum of the three resonances move progressively towards the threshold as the Cu concentration decreases.

The Cu $L_{3,2}$-edge XANES between the ordered and disordered phases of Cu_3Au and CuAu have also been recorded. The difference in E_0 between the ordered and the disordered phase is negligible within experimental uncertainty, although the resonance intensity for the disordered samples is slightly higher. The implication of this observation is noted in the next section.

IV. DATA ANALYSIS AND DISCUSSION

A. General considerations

In the absence of significant multielectron excitations that are not expected to be important in this system, the Cu $L_{3,2}$-edge XANES can be dealt with within the framework of the one-electron approximation. The difference in the final-state effect, which tends to induce screening charge of a more localized character (such as d charge), can be assumed to be small for this system. Thus the transition probability for the excitation of an electron from the Cu $2p_{3/2}$ level (L_3 edge) to the previously unoccupied states is governed by the
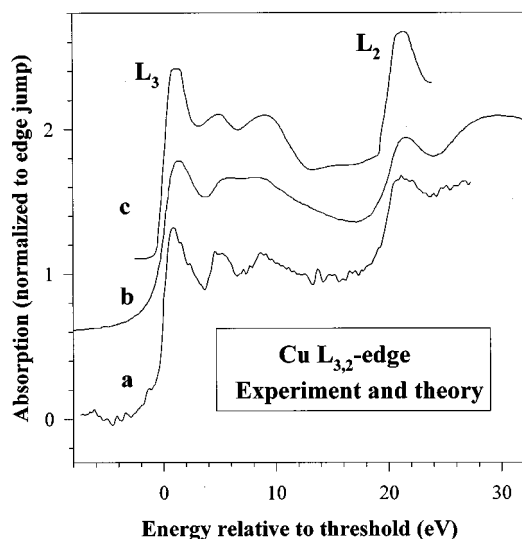
FIG. 2. Cu $L_{3,2}$-edge XANES: comparison of experiment (a, this work) with the theory of Muller (b, Ref. 17) and Aebi $et\ al.$ (c, Ref. 15).

dipole transition matrix element and the densities of the unoccupied states. Granted that the radial part of the transition matrix element varies very little from compound to compound and the $p \rightarrow d$ transition dominates, the unoccupied densities of d states can be probed with the $L_{3,2}$-edge XANES.[15,17,34,47,48,55–61]

The presence of unoccupied densities of d states above the Fermi level in Cu, Ag, and Au is supported by band theory and related calculations.[7,11,12,14,15,17,18] It has also been well established, both experimentally and theoretically, that metals with the same crystal structure exhibit similar patterns in their x-ray absorption fine structure.[16–18,20] Although there is less data length in the L_3 edge for Cu and Ni both fcc metals, it has been shown that they both exhibit a three-peak pattern.

Figure 2 compares the calculated and the experimentally observed Cu $L_{3,2}$-edge XANES for Cu metal. Spectrum a is the experimental data, while spectra b and c are calculations of Müller, Jepsen, and Wilkins[17] and Aebi $et\ al.$,[15] respectively, based on a band model. It is apparent from these results that all calculations correctly predict the three-peak pattern above the Cu L_3 edge, albeit with a small discrepancy in the energy position of the resonances. A recent calculation by Soldatov $et\ al.$[62] using multiple-scattering procedures[63,64] also correctly reproduces the three-peak pattern and shows

that $p \rightarrow d$ is the dominant contribution to the three-peak resonance of the Cu L_3-edge XANES; it is about an order of magnitude larger than that of the $p \rightarrow s$ contribution. Thus one expects that any change in the d electron count at the Cu site upon alloying would have a noticeable effect on the Cu $L_{3,2}$-edge XANES intensity. It has been shown that the Cu L_3 edge in Cu-Zr alloys exhibits an intense white line as the result of d charge depletion.[48]

B. Cu $L_{3,2}$-edge systematics for the disordered alloys

Let us first consider the polycrystalline, disordered fcc alloys with compositions of Cu_3Au, $CuAu$, and $CuAu_3$. We will examine the energy shifts of the threshold E_0, the relative position, and the intensity of the resonances relative to those of the pure metal.

It has been noted that the alloy E_0 shifts progressively to smaller photon energy relative to the pure metal as Cu becomes more dilute in the alloy. This observation is in good agreement with the trend found in the x-ray photoemission spectroscopy (XPS) study of the same series, which shows that the Cu $2p_{3/2}$ peak shifts to lower binding energy.[45] The relevant shifts are tabulated in Table I.

Figure 3 compares the Cu L_3-edge XANES of the disordered alloys with that of Cu metal. All spectra have been normalized to an edge jump of unity and the alloy spectra have been shifted so that the E_0 of the alloy spectrum is aligned with that of the pure metal. The normalization procedure was carried out by matching the absorption coefficients just below the L_3 threshold, below the L_2 threshold, and several eV above the L_2 threshold. The difference curve and the area under the difference curve, which is related to the unoccupied densities of d states, are also shown (shaded area).

A couple of interesting features from Fig. 3 are noted. First, despite the similarity in the three-resonance pattern, there are noticeable differences in both the position and the intensity of the resonances. Second, in the energy region of the first resonance ($\sim$first 5 eV) there is little or only a small change in intensity as Cu becomes more dilute, while the difference in the area under the second and the third resonance exhibits a significance decrease in alloys (the integrated absorption intensity decreases). The sum of the areas (including the sign) under the difference curve in the region of $\sim$10 eV above the threshold decreases and is dominated by changes under the second and the third resonance. This observation indicates a loss of intensity in the alloy compared to that of the pure Cu as Cu becomes more dilute. The

TABLE I. Chemical shift in the Cu L_3-edge threshold ΔE_0 and XPS Cu $2p_{3/2}$ binding energy ΔE_B for a series of disordered alloys relative to Cu metal

Alloy	E_0 (Cu L_3 edge)[a] (eV)	ΔE_0 (alloy Cu) (eV)	E_B ($2p_{3/2}$, XPS)[b] (eV)	ΔE_B (alloy Cu) (eV)
Cu	932.40(3)	0.0	932.53(3)	0.0
Cu_3Au	932.30(3)	−0.10(3)	932.33(3)	−0.20(3)
CuAu	932.21(3)	−0.19(3)	932.26(3)	−0.27(3)
$CuAu_3$	931.99(5)	−0.41(5)	932.18(3)	−0.38(3)

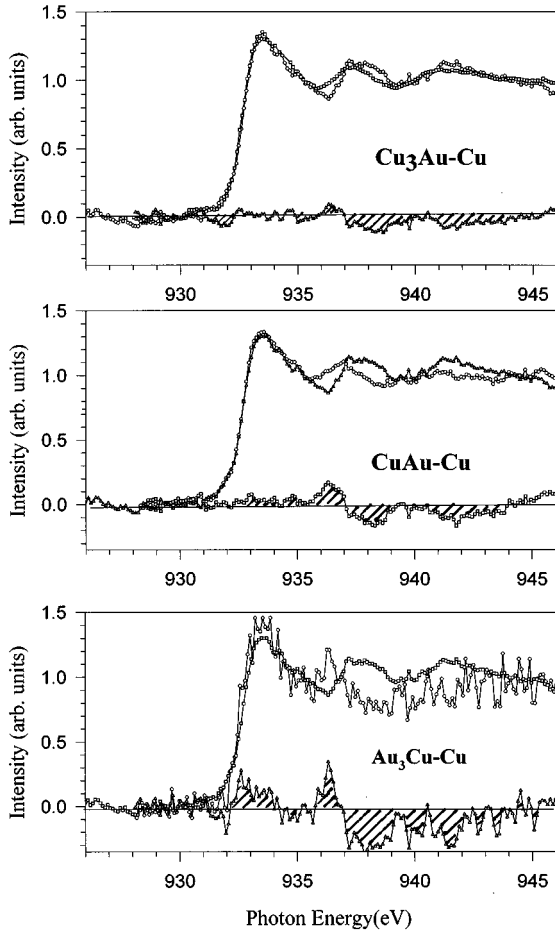[a]Relative to the Cu L_3-edge resonance maximum of CuO at 931.06 eV.
[b]From Ref. 45.

FIG. 3. Cu L_3-edge difference curve between disordered alloy and Cu; the area under the difference curve in the region of interest is shaded.

FIG. 4. Plots of XANES intensity (ΔA), Eo, and XPS ΔE_B vs alloy composition.

$$A_3 = C_0 N_0 E_3 (R_{2p\text{-}3d})^2 (6h_{5/2} + h_{3/2})/15, \qquad (2)$$

where C_0, N_0, and $E_{2,3}$ are constants. We consider only the L_3 edge here because the L_2 edge is complicated by the L_3-edge XAFS. From Eq. (2) we get

$$A(L_3) = a\{\tfrac{4}{9}[R_{2p\text{-}3d}]^2 h_{5/2}\} = a\{\tfrac{4}{15}[R_{2p\text{-}3d}]^2 h_d\}, \qquad (3)$$

where $a = C_0 N_0 E_3$ is a constant ($C_0 = 4\pi^2\alpha/3$, α being the fine-structure constant, N_0, the density of Cu atoms, and E_3 the Cu L_3 absorption edge energy) $R_{2p\text{-}3d} \sim R_{2p\text{-}3d}(2p_{3/2}\text{-}3d_{5/2,3/2}) \sim R_{2p\text{-}3d}(2p_{1/2}\text{-}3d_{3/2})$ is the radial transition matrix element, and h_d is the number of $5d$ holes. Thus the area under the difference curve between the alloy and Cu metal at the Cu L_3 edge becomes

$$\Delta A(L_3) = b\Delta h_d = -b\Delta n_d, \qquad (4)$$

where $b = a\left(\tfrac{4}{15}[R_{2p\text{-}3d}]^2\right)$ is a constant, Δh_d is the difference in $5d$ hole count between the alloy and the metal, and Δn_d is the difference in d electron count between the alloy and the metal. Equations (3) and (4) will form the basis for later discussions (Sec. IV C).

The chemical shifts E_0 and ΔE_B (from XPS) as well as changes in area under the curve $\Delta A(L_3)$ (henceforth denoted ΔA) of Fig. 3 are plotted as a function of composition in Fig. 4. Both chemical shift trends indicate that Cu gains charge upon alloying, while the ΔA trend indicates that Cu gains d charge.

We now recall previous observations for this series of alloys from the Au perspective.[45] It has been shown that Au gains s charge and loses d charge upon dilution in Cu and the d loss at the Au site (within the Wigner-Seitz volume) is overcompensated by the gain in s charge so that Au acquires a small net charge overall in forming the random alloy, in accord with electronegativity considerations. What follows, as required by charge conservation, is that Cu on the average must lose charge overall at the Cu site in these Cu-Au alloys. Since both XPS Cu $2p_{3/2}$ binding energy and Cu L_3-edge E_0 for the alloys exhibit a shift to lower binding energy upon dilution, this indicates that Cu gains d charge and loses s charge. This is because the Coulomb interaction between the

resonance maxima shift toward the threshold as Cu becomes more dilute. We tentatively attribute this shift to the localization of the d wave functions of Cu. Other relevant parameters are summarized in Table II.

Following Matthiess and Dietz for their studies of fcc Au and Pt (Ref. 14) and assuming there is no countervailing symmetry arguments when applied to fcc Cu, the integrated absorption intensity at the L_3 edge, A, is proportional to the number of $5d$ holes. Assuming statistical distribution of the d holes ($h_{5/2}/h_{3/2} = 1.5{:}1$; total hole count $h_d = h_{5/2} + h_{3/2}$), we can write

$$A_2 = C_0 N_0 E_2 (R_{2p\text{-}3d})^2 (h_{3/2})/3, \qquad (1)$$

TABLE II. Area under the Cu L_3-edge XANES difference curve between an alloy and Cu metal.

Alloy	ΔA^{a} (alloy Cu) unity edge jump (eV)	ΔA (alloy Cu) (eV cm^{-1})
Cu	0	0
Cu$_3$Au	-0.29	-7714
CuAu	-0.55	-14610
CuAu$_3$	-1.1	-29260

$^{\text{a}}$Unit in unity edge jump $\times$ (eV); for the Cu L_3 edge, the unity edge jump corresponds to 2.66×10^4 cm^{-1} (uncertainty $\leqslant 10\%$).
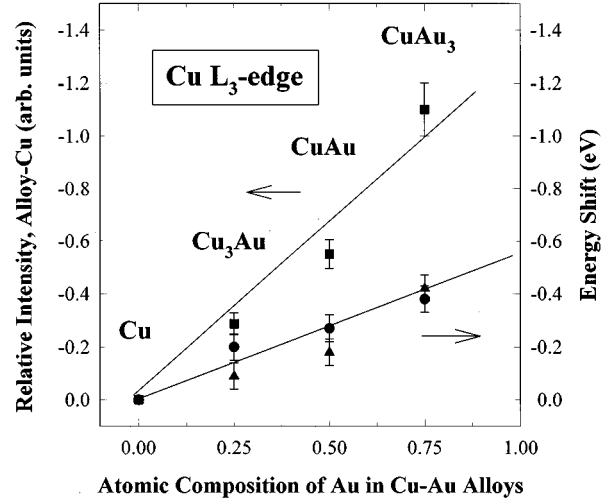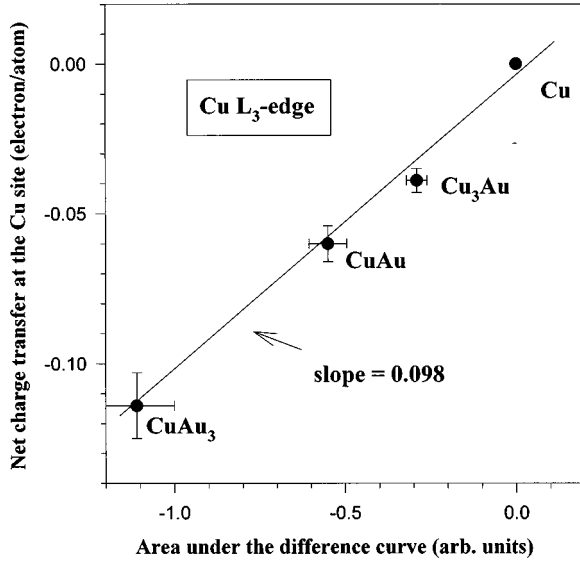
FIG. 5. Correlation of δ(Cu) with ΔA for the disordered alloys.

core electron and electrons in the $3d$ shell $F(2p,3d)$ is considerably larger than $F(2p,4s)$ (Ref. 65) [typical $F(2p,3d)$ values are ~ 10–20 eV across the $3d$ period and the $F(2p,3s)$ is typically 20% less]. Since the F's are the dominant terms that determine the binding energy shift, Cu in the alloy can still exhibit a negative-binding-energy shift despite a net charge loss if the depleted s is partially compensated by the gain of the more compact d charge.

We attribute the overall difference in the area under the curve in Fig. 3 to a gain of d charge at the Cu site in the alloys (decrease in d hole count). This assignment is partly based on the fact that the $p \rightarrow d$ transition is expected to be more sensitive than the $p \rightarrow s$ transition and partly based on the multiple-scattering calculation,[62] which shows that the three-peak pattern arises primarily from $p \rightarrow d$ transition. Thus the Cu $L_{3,2}$-edge XANES results support the notion that Cu gains d charge and loses s charge in forming Cu-Au alloys. It should be noted that the effect of p charge has so far been neglected. We assume that the p contribution is small and this assumption has been shown to be generally valid and its effect can be implicitly included in the s count.[46]

C. Comparison with previous Au results and theoretical calculations

We now attempt to quantify these observations. Let us consider for the moment the area under the Cu L_3-edge difference curve ΔA. We can rewrite Eq. (4) as

$$\Delta n_d = c \Delta A, \qquad (5)$$

where $c = -1/b$ is a proportional constant. We now impose charge conservation, which demands that

$$i\,\delta(\text{Cu}) = \delta(\text{Au}), \qquad (6)$$

where i is the atomic ratio of Cu to Au in the alloy and δ is the net charge transfer on or off the site (Wigner-Seitz volume) of interest. Using δ(Au) values from a previous study for these exact alloy samples,[45] we can estimate δ(Cu) from

$$\delta(\text{Cu}) = \Delta n_s + \Delta n_d. \qquad (7)$$

Assuming that $\Delta n_s / \Delta n_d = r$ is a constant as in the case of Au,[45] we arrive at

$$\delta(\text{Cu}) = (r+1)\Delta n_d, \qquad (8)$$

which, when combined with Eq. (5), yields

$$\delta(\text{Cu}) = c(r+1)\Delta A. \qquad (9)$$

If all the above assumptions are valid, we then expect to observe a liner relationship between δ(Cu) and ΔA. The relevant data are given in Table III and the results are shown in Fig. 5. It can be seen from Fig. 5 that the correlation is linear, yielding a slope of $c(r+1)=0.098$. If we take $r=-1.43$, which is the same as in the case of Au (Ref. 45) (this is an upper bound, r is expected to be closer to -1 in Cu), we obtain $c=-0.228$ (if we take $r=-1.2$, c becomes -0.49). Returning to Eq. (5), we can now estimate Δn_d values from ΔA. The values thus obtained are listed in Table III. We can see from Table III that these values are of the order of 0.1 electron and increases as Cu becomes more dilute.

A theoretical calculation addressing charge transfer in Cu-Au alloys in general is lacking, except in the case of Cu_3Au. In the linear muffin-tin orbital coherent potential approximation calculation of Abrikosov, Vekilov, and Ruban,[11] they show that Au loses d and gains s for both ordered and disordered alloys, while the d count at the Cu site changes very little. Lu $et\ al.$,[10] using a special quasirandom structure method, have calculated the charge transfer in both ordered and disordered Cu_3Au. They found that the integrated total charge transfer inside the muffin-tin sphere of Cu and Au in Cu_3Au exhibits the following trends: (a) Au loses charge and Cu gains charge; (b) the charge depletion at the Au site amounts to 0.4–0.5 e/atom, depending on the number of nearest like atoms (the larger the number, the smaller the charge transfer); and (c) the charge gain at the Cu site is relatively small (0.01 and 0.08 e/atom for 11 and 7 nearest like neighbors, respectively). It should be noted that charge-

TABLE III. Charge transfer at the Au and Cu sites for a series of random alloys.

Alloy	δ (Au)[a]	Δn_d (Au)[a]	δ (Cu)[b]	Δn_d (Cu)[c]	ΔA (Cu L_3)
Cu_3Au	0.11_7	-0.13_3	-0.03_9	0.06_6	-0.29 ± 0.03
$CuAu$	0.06_0	-0.06_7	-0.6_0	0.12_5	-0.55 ± 0.06
$CuAu_3$	0.03_8	-0.02_2	-0.11_4	0.25_1	-1.10 ± 0.11

[a]From Ref. 45.

[b]Calculation based on charge conservation; see text.

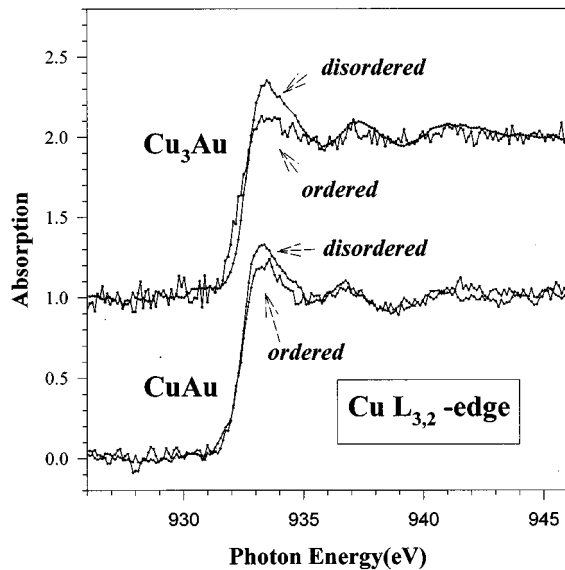[c]From Eq. (5); uncertainty primarily originates from ΔA (slightly different background subtraction and normalization).

FIG. 6. Comparison of the Cu L_3-edge XANES between the ordered and the disordered Cu_3Au and CuAu.

FIG. 7. Comparison of K- and $L_{3,2}$-edge XANES for Cu metal.

transfer consideration based on a muffin-tin sphere is different from our consideration (Wigner-Seitz volume). Conceptually, it is easier to visualize charge transfer if all the volumes are accounted for. Consequently, charge conservation is imposed automatically. However, the Wigner-Seitz volume is more difficult to deal with than the muffin tin in theoretical calculations. We tend to interpret the charge transfer within the muffin-tin sphere as charges of a more compact (localized) character. Then our results are in good agreement with theory[10] and indicate that Cu gains d charge, while Au loses d and gains s charge upon alloying. The role of Cu s charge is less clear, although charge conservation requires that Cu should lose conduction charge.

Returning to Eq. (4), we can also estimate the radial matrix element $R_{2p\text{-}3d}$ for Cu. Using $\Delta n_d = 0.125$ for CuAu from Table III and $C_0 = 9.605 \times 10^{-2}$, $E_3 = 932.4$ eV, and $N_0 = 8.474 \times 10^{24}$ atom cm^{-3}, we obtain $a = 7.589 \times 10^{24}$ eV cm^{-3} and an $R_{2p\text{-}3d}$ value of 1.44×10^{-10} cm. This value has the same order of magnitude as that reported by Pearson[48] (6.4×10^{-10} cm) using atomic calculations, but is about four times smaller. The discrepancy may be due to an overestimate of the r value used in the analysis. An r value of -1.2 would yield an $R_{2p\text{-}3d}$ value of 3.1×10^{-10} cm, which shows a much better agreement between experiment and calculation.

D. Cu L_3-edge XANES for ordered and disordered Cu_3Au and CuAu

Of all the Cu-Au alloys, the ordered-disordered phase transitions of Cu_3Au and CuAu are undoubtedly the ones that have drawn the most attention. We present below some Cu L_3-edge observations and their qualitative implications. More detailed study is presently under way and will be given elsewhere.

Figure 6 shows an expanded region of the Cu L_3-edge XANES for the ordered and disordered samples of Cu_3Au and CuAu. It is apparent from Figs. 6 and 3 that the intensi-

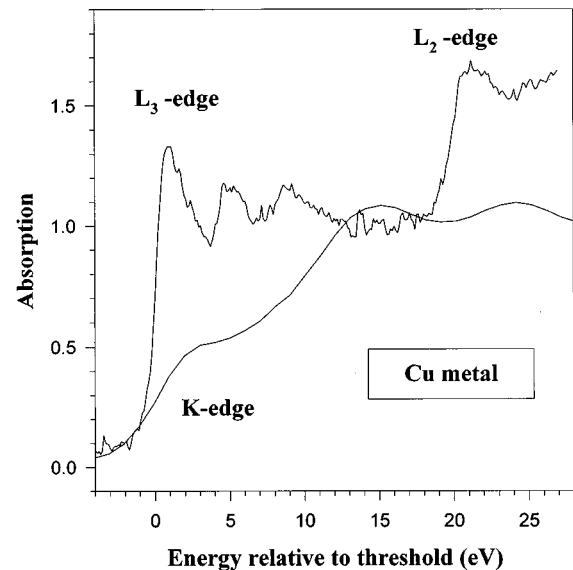ties of the three-peak resonance region exhibit the following trend: Cu$>$Cu$_3$Au (disordered)$>$Cu$_3$Au (ordered). This trend, which follows the number of nearest neighbors of like atoms, is, however, exactly opposite that exhibited by the Au $L_{3,2}$-edge white line of the same alloys.[45] A similar pattern is also found for the CuAu alloys. These results confirm qualitatively what the photoemission and threshold chemical shift already indicated, that Cu gains more d charge when it is more dilute locally in Au. It should be noted that, on average, both Au and Cu are less dilute locally (larger number of nearest neighbor of like atoms) in the random alloy than in the ordered structure of Cu_3Au ($L1_2$) and CuAu ($L1_0$). Au has no nearest Au neighbors in the ordered Cu_3Au ($L1_2$) structure, but has three nearest Au neighbors in the disordered fcc structure on average, while Cu has eight nearest Cu neighbors in the ordered structure and nine Cu neighbors on average in the disordered structure. In the case of CuAu, both Au and Cu have four nearest like neighbors in the ordered structure ($L1_0$), while the coordination number is six on average in the disordered structure. The trend observed here is entirely consistent with the notion that the more dilute Cu(Au) is in Au(Cu) locally, the more d electrons it gains (loses).[45]

E. Comparison of Cu L_3-edge with Cu K-edge XANES

It is also interesting to compare the Cu L-edge XANES result with that of the Cu K edge. Figure 7 plots the K- and $L_{3,2}$-edge XANES of Cu metal with both E_0 set at zero. The absorption coefficients have been normalized to unity edge jump. The effects of the core-hole lifetime and angular momentum characteristics (selection rules $\Delta l = \pm 1$, $\Delta j = 0, \pm 1$) on the XANES features are immediately apparent. A couple of interesting features are also noted. First, the spectra look entirely different, as expected, since the K-edge XANES probes the $l = 1$ (p) state and the L_3 edge probes the $l = 0$ (s) and 2 (d) states, with the latter being the dominant process. Second, the shoulder in the K-edge XANES, which has been interpreted as an $s \rightarrow d$ transition facilitated by band forma-

tion and rehybridization,[17,45] is relatively weak and falls in the same energy region (~ 10 eV) as that probed by the L_3 edge.

V. SUMMARY AND CONCLUSIONS

We have reported the study of high-resolution Cu L_3-edge XANES spectra for a series of disordered Cu-Au alloys as well as a preliminary study of the ordered Cu_3Au and CuAu. The XANES spectra clearly show chemical systematics that have been interpreted in terms of d charge redistribution at the Cu site. These results, together with previously reported Au results and theoretical calculations, strongly indicate that relative to the pure metal, Cu gains d charge and Au loses d charge in Cu-Au alloys. The trends of d charge redistribution at the Cu and Au sites are in opposite directions and are in contrast to what is expected on the basis of electronegativity arguments. We proposed that this discrepancy could be resolved by the introduction of the charge compensation mechanism, which allows for s charge compensation. The result then is that Cu gains d and loses s charge, while Au loses s and gains d and that the net charge flow is small and is onto Au and off Cu in accord with electronegativity and electroneutrality arguments. Results from both disordered and ordered alloys show that d charge redistribution at the site is intimately related to the number of nearest neighbors of like (unlike) atoms. This result supports an earlier notion that the number of nearest neighbors of like atoms is more important to the electronic structure than the interatomic distance between them.[45] In addition, we have also estimated the $R_{2p\text{-}3d}$ value for Cu and compared the Cu L_3- and K-edge XANES, showing that the atomiclike dipole selection rule is generally valid and that the first ~ 10 eV above the threshold is important for unoccupied densities of states considerations in these systems. Finally, it should be noted that we have addressed here only the phenomenological correlation between the area under the difference curve and charge transfer. The origin of the chemical sensitivity of the three-peak pattern in the context of densities of states (band model) and resonance states (multiple-scattering considerations) and their relationship to charge transfer need further study. Future study with new generation of monochromators that provide still better resolution and with calculations involving the core hole will undoubtedly shed more light on these issues.

---

*Present address: Department of Materials Science, Hiroshima University, Hiroshima 730, Japan.

†Present address: Institute for Scientific Measurements, Tohuko University, Sendi 980, Japan.

[1] The techniques in question are photoemission and x-ray-absorption spectroscopy using synchrotron radiation; see Refs. 2 and 3 for the status of these techniques and their applications.

[2] Proceedings of the SRI 94 International Conference [Rev. Sci. Instrum. **66** (1995)].

[3] Proceedings of the International Conference XAFS8 [Physica B **208&209** (1995)].

[4] R. E. Watson, J. W. Davenport, and M. Weinert, Phys. Rev. B **35**, 508 (1987).

[5] J. W. Davenport, R. E. Watson, and M. Weinert, Phys. Rev. B **37**, 9985 (1988).

[6] B. Ginatempo and J. B. Staunton, J. Phys. F **18**, 1827 (1988).

[7] P. Weinberger, A. M. Boring, R. C. Albers, and W. M. Temmerman, Phys. Rev. B **38**, 5357 (1988).

[8] E. Arola, R. S. Rao, A. Salokatve, and A. Bansil, Phys. Rev. B **41**, 7361 (1990).

[9] B. Ginatempo, G. Y. Guo, W. M. Temmerman, J. B. Staunton, and P. J. Durham, Phys. Rev. B **42**, 2761 (1990).

[10] Z. W. Lu, S.-H. Wei, A. Zunger, S. Frota-Pessoa, and L. G. Ferreira, Phys. Rev. B **44**, 512 (1991).

[11] I. A. Abrikosov, Yu. H. Vekilov, and A. R. Ruban, Phys. Lett. A **154**, 407 (1991).

[12] Z. W. Lu, S. H. Wei, and A. Zunger, Phys. Rev. B **45**, 10 314 (1992).

[13] M. Brown, R. E. Peierls, and E. A. Stern, Phys. Rev. B **15**, 738 (1977).

[14] L. F. Mattheiss and R. E. Dietz, Phys. Rev. B **22**, 1663 (1980).

[15] P. Aebi, M. Erbudak, F. Vanini, D. D. Vvedensky, and G. Kos-

torz, Phys. Rev. B **41**, 11 760 (1981).

[16] G. Van der Laan, C. Westra, C. Hass, and G. A. Swatzky, Phys. Rev. B **23**, 4369 (1981).

[17] J. E. Muller, O. Jepsen, and J. W. Wilkins, Solid State Commun. **42**, 365 (1982).

[18] V. V. Nemoshkalenno, V. N. Anfonov, V. I. N. Antonov, W. John, H. Wonn, and P. Ziesche, Phys. Status Solidi B **111**, 11 (1982).

[19] A. Bianconi, J. Garcia, and M. Benfatto, in *Synchrotron Radiation in Chemistry and Biology I*, edited by E. Mandelkow, Topics in Current Chemistry Vol. 145 (Springer-Verlag, Berlin, 1988), p. 29.

[20] *Unoccupied Densities of States*, edited by J. C. Fuggle and J. E. Inglefield (Springer-Verlag, Berlin, 1993), and reference therein.

[21] C. T. Campbell, Annu. Rev. Phys. Chem. **41**, 775 (1990).

[22] J. A. Rodriguez and D. W. Goodman, Science **257**, 897 (1992).

[23] J. C. Vickerman, K. Christmann, G. Ertl, P. Heimann, F. J. Himpsel, and D. Eastman, Surf. Sci. **134**, 367 (1983).

[24] J. E. Houston, C. H. F. Peden, P. J. Feibelman, and D. R. Hamann, Phys. Rev. Lett. **56**, 375 (1986); Surf. Sci. **195**, 457 (1987).

[25] C. Harendt, K. Christmann, W. Hirschwald, and J. C. Vickerman, Surf. Sci. **165**, 413 (1986).

[26] C. Park, E. Bauer, and H. Poppa, Surf. Sci. **187**, 86 (1987).

[27] J. W. Niemantsverdriet, P. Dolle, K. Markert, and K. Wandelt, J. Vac. Sci. Technol. A **5**, 875 (1987).

[28] K. Kalki, B. Pennemann, U. Schröder, W. Heichler, and K. Wandelt, Appl. Sur. Sci. **48/49**, 59 (1991); M. Schick, J. Schäfer, K. Kalki, G. Ceballos, P. Reinhardt, H. Hoffschulz, and K. Wandelt, Sur. Sci. **287/288**, 960 (1993).

[29] M. Kuhn, Z. H. Lu, and T. K. Sham, Phys. Rev. B **45**, 3703 (1992).

[30] M. Kuhn, A. Bzowski, T. K. Sham, J. A. Rodriguez, and J. Hrbek, Thin Solid Films **283**, 209 (1996).

[31] T. K. Sham, T. Ohta, T. Yokoyama, Y. Kitajima, M. Funabashi, N. Kosugi, and H. Kuroda, J. Chem. Phys. **88**, 475 (1988); T. K. Sham, Z.-F. Liu, and K. H. Tan, *ibid*. **94**, 6250 (1991).

[32] T. K. Sham, J. Hrbek, and K. H. Tan, Surf. Sci. **236**, 259 (1990).

[33] J. H. Sinfelt, *Bimetallic Catalysts* (Wiley, New York, 1983); Rev. Mod. Phys. **51**, 569 (1979).

[34] T. K. Sham, I. Coulthard, J. W. Lorimer, A. Hiraya, and M. Watanabe, Chem. Mater. **6**, 2085 (1994).

[35] P. H. Barrett, R. W. Grant, M. Kaplan, D. A. Keller, and D. A. Shirley, J. Chem. Phys. **39**, 1035 (1963); L. D. Roberts, J. O. Thomson, and P. G. Huray, Phys. Rev. **129**, 664 (1963); L. D. Roberts, R. L. Becker, F. E. Obenshain, and J. O. Thomson, *ibid*. **137**, A895 (1965); P. G. Huray, L. D. Roberts, and J. O. Thomson, Phys. Rev. B **4**, 2147 (1971); F. E. Wagner, G. Wortmann, and G. M. Kalvis, Phys. Lett. **42A**, 483 (1973).

[36] T. K. Sham, R. E. Watson, and M. L. Perlman, Adv. Chem. Ser. **194**, 39 (1981).

[37] M. Kuhn, A. Bzowski, and T. K. Sham, Hyperfine Interact. **94**, 2267 (1994).

[38] R. E. Watson, J. Hudis, and M. L. Perlman, Phys. Rev. B **4**, 4139 (1971).

[39] W. Eberhardt, S. C. Wu, R. Garrett, D. Sondericker, and F. Jona, Phys. Rev. B **31**, 8285 (1985).

[40] S. B. DiCenzo, P. H. Citrin, E. H. Harford, Jr., and G. K. Wertheim, Phys. Rev. B **34**, 1343 (1986).

[41] Z. Q. Wang, Y. S. Li, C. K. C. Lok, J. Quinn, F. Jona, and P. M. Marcus, Solid State Commun. **62**, 181 (1987).

[42] G. W. Graham, Surf. Sci. **184**, 137 (1987).

[43] J. C. Hansen, J. A. Benson, W. D. Clendening, M. T. McEllistrem, and J. G. Tobin, Phys. Rev. B **36**, 6186 (1987).

[44] T. K. Sham, Y. M. Yiu, M. Kuhn, and K. H. Tan, Phys. Rev. B **41**, 11 881 (1990).

[45] M. Kuhn and T. K. Sham, Phys. Rev. B **49**, 1647 (1994).

[46] T. K. Sham, M. L. Perlman, and R. E. Watson, Phys. Rev. B **19**, 539 (1979).

[47] R. D. Leapman and L. A. Grune, Phys. Rev. Lett. **45**, 397 (1980).

[48] D. H. Pearson, Ph.D. thesis, California Institute of Technology, 1992, and references therein; D. H. Pearson, B. F. Fultz, and C. C. Ahn, Appl. Phys. Lett. **53**, 1405 (1988).

[49] High-resolution grating monochromators operating in the 1-keV photon energy range were discussed extensively in Proceedings of the SRI 91 International Conference [Rev. Sci. Instrum. **63**(2) (1992)].

[50] T. Cleason and J. B. Boyce, Phys. Rev. B 1551 (1984).

[51] A. Hiraya, T. Horigome, N. Okada, N. Mizutani, K. Sakai, O. Matsudo, M. Hasumota, K. Fukui, and M. Watanabe, Rev. Sci. Instrum. **63**, 1264 (1992).

[52] A. Hiraya, M. Watanabe, and T. K. Sham, Rev. Sci. Instrum. **66**, 1528 (1995).

[53] Electrons primarily responsible for the TEY are the Cu LVV Auger (<900 eV) and secondary electrons (energy distribution maximum ~15 eV). These electrons would have an escape depth of the order of 1 nm according to the universal curve of attenuation length of electron in solids. For details see A. Erbil, G. S. Cargill III, R. Frahm, and R. F. Boehme, Phys. Rev. B **37**, 2450 (1988).

[54] The total absorption coefficient of Cu at the Cu L fluorescent x-ray energy (~930 eV) is 1.59×10^3 cm^2/g according to Henke *et al.*, At. Data Nucl. Data Tables **27**, 1 (1982). The corresponding $1/e$ attenuation length of the soft x rays by Cu is 700 nm.

[55] G. Meitzner, D. A. Fischer, and J. H. Sinfelt, Catal. Lett. **5**, 219 (1992).

[56] A. N. Mansour, J. W. Cook, Jr., and D. E. Sayers, J. Phys. Chem. **88**, 2330 (1984).

[57] C. C. Tyson, A. Bzowski, P. Kristof, R. Sammyreiken, M. Kuhn, and T. K. Sham, Phys. Rev. B **45**, 8811 (1992).

[58] T. K. Sham, Phys. Rev. B **13**, 1903 (1985).

[59] J. Chen, M. Croft, X. Xu, S. A. Shaheen, and F. Lu, Phys. Rev. B **46**, 15 639 (1992).

[60] A. Bzowski, Y. M. Yiu, and T. K. Sham, Jpn. J. Appl. Phys. Suppl. 2 **32**, 691 (1993); A. Bzowski, T. K. Sham, and Y. M. Yiu, Phys. Rev. B **49**, 13 776 (1994).

[61] F. W. Lytle, Ber. Bunsenges. Phys. Chem. **91**, 1251 (1987).

[62] A. V. Soldatov *et al.* (unpublished).

[63] S. Della Longa, A. V. Soldatov, M. Pompa, and A. Bianconi, Comput. Sci. (to be published).

[64] P. Durham, in *X-Ray Absorption: Principles, Applications, Techniques for EXAFS, SEXAFS, and XANES*, edited by D. C. Kroningsberger and R. Prins (Wiley, New York, 1988), p. 53.

[65] R. E. Watson and M. L. Perlman, Struct. Bonding **24**, 83 (1975).